J Neurophysiol 113: 2605–2617, 2015.
First published February 4, 2015; doi:10.1152/jn.00480.2014.

Surround suppression and temporal processing of visual signals

Henry J. Alitto[1,2] and W. Martin Usrey[1,2,3]

[1]*Center for Neuroscience, University of California-Davis, Davis, California;* [2]*Department of Neurobiology, Physiology, and Behavior, University of California-Davis, Davis, California; and* [3]*Department of Neurology, University of California-Davis, Sacramento, California*

Submitted 3 July 2014; accepted in final form 3 February 2015

Alitto HJ, Usrey WM. Surround suppression and temporal processing of visual signals. *J Neurophysiol* 113: 2605–2617, 2015. First published February 4, 2015; doi:10.1152/jn.00480.2014.—Extraclassical surround suppression strongly modulates responses of neurons in the retina, lateral geniculate nucleus (LGN), and primary visual cortex. Although a great deal is known about the spatial properties of extraclassical suppression and the role it serves in stimulus size tuning, relatively little is known about how extraclassical suppression shapes visual processing in the temporal domain. We recorded the spiking activity of retinal ganglion cells and LGN neurons in the cat to test the hypothesis that extraclassical suppression influences temporal features of visual responses in the early visual system. Our results demonstrate that extraclassical suppression not only shifts the distribution of interspike intervals in a manner that decreases the efficacy of neuronal communication, it also decreases the reliability of neuronal responses to visual stimuli and it decreases the duration of visual responses, an effect that underlies a rightward shift in the temporal frequency tuning of LGN neurons. Taken together, these results reveal a dynamic relationship between extraclassical suppression and the temporal features of neuronal responses.

cat; lateral geniculate nucleus; extraclassical suppression; nonlinear receptive field

GAIN CONTROL MECHANISMS, including extraclassical surround suppression, are a prominent feature of visual responses in the retina and lateral geniculate nucleus (LGN), providing nonlinear modulation to otherwise linear receptive fields (Baccus and Meister 2002; Bonin et al. 2005; Enroth-Cugell and Robson 1966; Murphy and Sillito 1987; Scholl et al. 2012; Sclar 1987; Shapley and Victor 1979b). Past work examining the spatial organization of these nonlinear mechanisms demonstrates that the suppressive influence of gain control becomes increasingly prominent as the size of the visual stimulus increases, resulting in the phenomenon commonly referred to as extraclassical surround suppression (Alitto and Usrey 2008; Camp et al. 2009; Hubel and Wiesel 1961; Solomon et al. 2002). Importantly, extraclassical suppression cannot be explained by the classical, center-surround receptive field structure (Alitto and Usrey 2008; Bonin et al. 2005; Shapley and Victor 1979b). Although a great deal is known about the spatial properties of extraclassical suppression, relatively little is known about its influence on the temporal features of neuronal responses. Perceptually, nonlinear influences of stimulus intensity are correlated with changes in the duration of human visual impulse responses (Georgeson 1987; Stromeyer and Martini 2003; Tadin et al. 2006), and suppressive surround mechanisms influence the temporal dynamics of center processing (Tadin et al. 2003). Given these reported effects and the prominence of suppression in the visual system, we performed experiments to determine the influence of extraclassical suppression on the temporal features of visual responses in the cat retina and LGN.

Although multiple circuits are implicated in the generation of surround suppression, surround suppression has been successfully integrated into a unified framework with several other seemingly disparate features of nonlinear gain control commonly referred to as retinal contrast gain control (Bonin et al. 2005; Felisberti and Derrington 1999; Mante et al. 2008; Shapley and Victor 1979b; Solomon et al. 2002; Usrey and Reid 2000). As originally described by Shapley and colleagues, the gain of many retinal ganglion cells and LGN neurons is not constant but instead decreases as stimulus contrast increases (illustrated in Fig. 1, *A* and *B*), causing contrast response functions to saturate at high contrasts. The temporal properties of retinal ganglion cells and LGN neurons are also dependent on stimulus contrast; response durations and latencies decrease and neurons become more responsive to higher temporal frequencies as stimulus contrast increases (illustrated in Fig. 1, *C–F*). As such, there is a key prediction that surround suppression, like retinal gain control, should decrease the duration of neuronal responses to visual stimuli and shift the temporal frequency tuning of neurons toward higher frequencies. Proposed mechanisms underlying these nonlinear phenomena include divisive inhibition and conductance-based changes in temporal dynamics (Ayaz and Chance 2009; Carandini and Heeger 2011; Murphy and Miller 2003).

Understanding the influence of surround suppression in the temporal domain is important, as the timing of visual activity is likely to have dramatic effects on both the strength of interneuronal communication and the ability of neurons to follow dynamic stimuli. Surround suppression is predicted to influence neuronal communication by shifting the distribution of interspike intervals (ISIs) toward greater values. Because retinal spikes are most effective in driving LGN action potentials when they are preceded by short ISIs compared with long ISIs (Levine and Cleland 2001; Mastronarde 1987; Rathbun et al. 2010; Sincich et al. 2007; Usrey et al. 1999; Weyand 2007), extraclassical suppression is predicted to reduce the efficacy of individual spikes in evoking postsynaptic responses and restructure the temporal organization of spikes delivered to downstream targets (reviewed in Usrey 2002).

In this study, we examined the influence of surround suppression on the temporal features of visual responses in the retina and LGN. Results reveal that surround suppression interacts with ISI-based mechanisms to adjust the strength of interneuronal communication in a manner that progressively amplifies the relative magnitude of suppression in the retina, LGN, and primary visual cortex (V1). Surround suppression

Address for reprint requests and other correspondence: W. M. Usrey, Center for Neuroscience, Univ. of California-Davis, 1544 Newton Ct., Davis, CA 95618 (e-mail: wmusrey@ucdavis.edu).

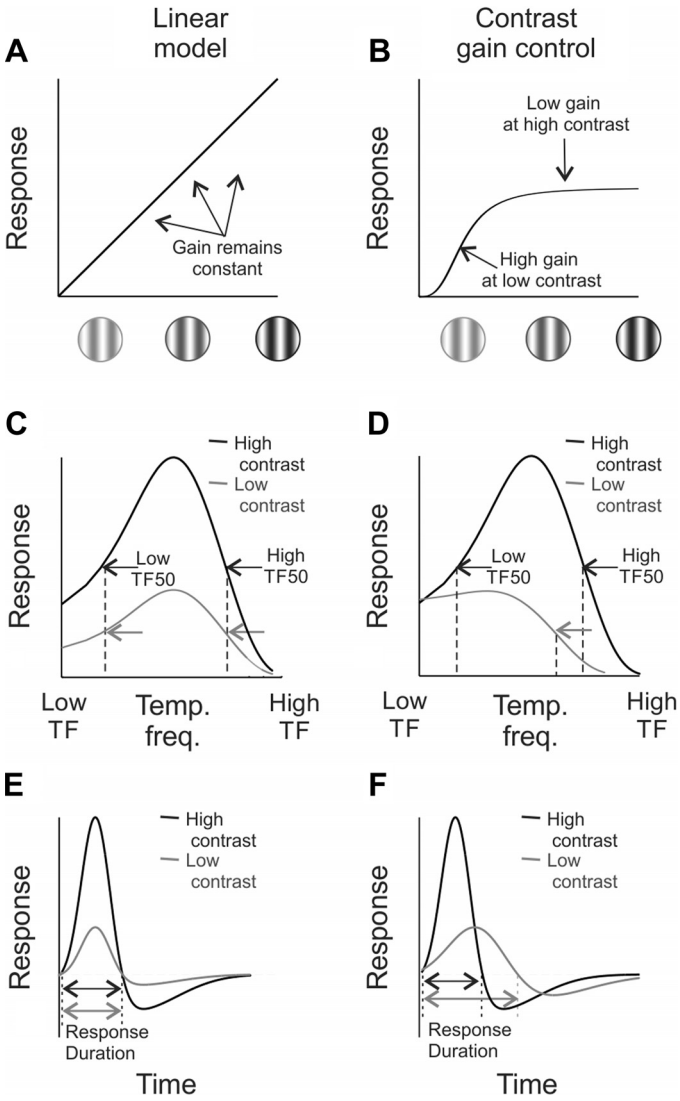

Fig. 1. Contrast gain control in the retina and lateral geniculate nucleus (LGN). *A*: the response of a hypothetical linear retinal ganglion cell or LGN neuron as a function of stimulus contrast. Gain is constant regardless of the strength of the visual stimulus. *C* and *E*: likewise, the temporal frequency (TF) response function (*C*) and impulse response (*E*) of a linear LGN neuron simply scale with stimulus contrast. Thus measures like the TF50 and response duration remain constant as contrast changes (black line, high contrast; gray line, low contrast). *B*: the response gain of many real LGN neurons, however, decreases as stimulus contrast increases, a phenomenon known as contrast gain control. *D* and *F*: furthermore, the temporal frequency response function (*D*) and impulse response (*F*) of many LGN neurons are significantly transformed as stimulus contrast increases, becoming less sensitive to low frequencies and more sensitive to high frequencies.

also has a significant influence on response reliability, the time course of impulse response functions, and the temporal frequency tuning of LGN neurons. These results collectively demonstrate that the nonlinear surround is much more than a spatial receptive field property; it plays a major role in systematically transforming temporal features of visual signals en route from the retina to the visual cortex.

MATERIALS AND METHODS

Surgery and preparation. Single-unit recordings were made from LGN neurons in 13 adult cats (both sexes). All surgical and experimental procedures conformed to National Institutes of Health guidelines and were carried out with the approval of the Animal Care and Use Committee at the University of California-Davis. Surgical anesthesia was induced with ketamine (10 mg/kg im) and maintained with thiopental sodium (20 mg/kg iv, supplemented as needed). Animals received a tracheotomy and were placed in a stereotaxic apparatus where temperature, ECG, EEG, and expired CO_2 were monitored continuously throughout the experiment. The level of anesthesia was maintained by a continuous infusion of thiopental sodium (2–3 $mg \cdot kg^{-1} \cdot h^{-1}$ iv). If physiological monitoring indicated a low level of anesthesia, additional thiopental was given and the rate of continuous infusion increased.

A midline scalp incision was made, and wound margins were infused with lidocaine. A small craniotomy was made above the LGN and/or optic tract, and the dura was removed. The eyes were secured to posts attached to the stereotaxic frame to minimize eye movements, fitted with appropriate contact lenses, and focused on a tangent screen located 172 cm in front of the animal. The positions of area centralis and the optic disk were plotted by back-projecting the retinal vasculature of each eye onto the tangent screen. Once all surgical procedures were complete, animals were paralyzed with vecuronium bromide (0.2 $mg \cdot kg^{-1} \cdot h^{-1}$ iv) and mechanically respired.

Data acquisition and visual stimuli. Recordings were made from neurons in layers A and A1 of the LGN or from the axons of retinal ganglion cells in the optic tract with Parylene-coated tungsten electrodes (A-M Systems, Everett, WA) or borosilicate glass-coated tungsten electrodes (Theodore Weyand, LSU Medical Center), respectively. Neuronal responses were amplified, filtered, and recorded to a PC equipped with a Power 1401 data acquisition interface and the Spike 2 software package (Cambridge Electronic Design, Cambridge, UK). Spike isolation was based on waveform analysis and the presence of a refractory period, as indicated by the autocorrelogram (Alitto et al. 2005).

Visual stimuli were created with a VSG2/5 visual stimulus generator (Cambridge Research Systems, Rochester, UK) and presented on a gamma-calibrated Sony monitor running at 140 Hz. The mean luminance of the monitor was 38 cd/m^2. Visual responses of LGN neurons and optic tract fibers were characterized quantitatively with drifting and contrast-reversing sinusoidal gratings (described below). Drifting gratings were shown for 4 s, followed by 4 s of mean gray. Contrast-reversing gratings were shown for 3 s, followed by 2 s of mean gray. For drifting gratings firing rate is reported as the first harmonic of the temporal frequency, while mean firing rate is reported for all other, nonperiodic stimuli. Because surround suppression is maximal with high-contrast stimuli (Bonin et al. 2005; Sceniak et al. 2006) and contrast gain control mechanisms occur across the range of stimulus contrast, including high contrasts (Bonin et al. 2005; Felisberti and Derrington 1999; Mante et al. 2008; Shapley and Victor 1979b; Solomon et al. 2002), all recordings were made while neurons were excited with high-contrast stimuli (100%; Michelson contrast).

Classical receptive field response properties. For each cell, the center of the receptive field was localized with a custom mapping program, utilizing a mouse-controlled drifting sine-wave grating. The center of the receptive field was determined by reducing the size of the grating to the smallest diameter (typically 0.1–0.3°) to evoke an audible change in firing rate. With this diameter, the center was set as the location that evoked the maximal firing rate. This process was repeated two or three times to ensure accuracy. Next the preferred spatial frequency was determined by presenting full-field drifting sine-wave gratings (4 Hz) of various spatial frequencies (typically 12 frequencies from 0.1 to 3.0 cycles/°) repeated three times each (4-s presentations followed by 4 s of mean gray).

Area summation response functions. To determine the relationship between stimulus diameter and neuronal firing rate, drifting sine-wave gratings (4 Hz, preferred spatial frequency) of various diameters (typically 20 sizes, logarithmically spaced between 0.1° and 10°) were presented centered over the receptive field of the neuron under

investigation. The responses evoked by these stimuli were then fit to a difference of Gaussians (DOG) equation:

$$R(x) = K_c \times \sum_{-x2}^{x2} \exp\left(-\left(2 \times x/r_c\right)^2\right) - K_s \times \sum_{-x2}^{x2} \exp\left(-\left(2 \times x/r_s\right)^2\right)$$

where $R(x)$ is the response evoked by diameter x, K_c is the amplitude of the center subunit, r_c is the radius of the center subunit, K_s is the amplitude of the surround subunit, and r_s is the radius of the surround subunit. The surround subunit radius was taken to be the spatial extent of the extraclassical receptive field. A suppression index was used to quantify the amount of suppression with the equation

$$\text{Suppression Index} = 1 - \frac{\text{Response to large grating (at plateau of DOG fit)}}{\text{Response to optimal grating (at peak of DOG fit)}}$$

Linear vs. nonlinear contributions to surround suppression. To accomplish the goal of characterizing the influence of nonlinear suppression on the temporal response properties of LGN neurons, it was essential to first estimate the contribution of linear mechanisms from the classical receptive field to what would otherwise be mistaken as nonlinear suppression. We began by assuming a DOG spatial profile for each LGN neuron in our data set (Fig. 2, *A–C*; Rodieck 1965). With this assumption, the spatial parameters of the classical center and surround were estimated by fitting a spatial frequency response function to a frequency domain DOG equation (DOG_f; Fig. 2*C*; Alitto and Usrey 2008; So and Shapley 1981):

$$SF_{(x)} = K_c \times \exp\left(-1 \times \left(\text{pi} \times r_c \times x\right)^2\right) - K_s \times \exp\left(-1\left(\text{pi} \times r_s \times x\right)^2\right)$$

where K_c and K_s are the amplitudes of the classical center and surround, respectively, and r_c and r_s are the radii of the classical center and surround, respectively.

The contribution of linear mechanisms to the measured surround suppression depends on the visual stimulus used to measure the area summation response function. Linear suppression will occur when there is a mismatch between the visual stimulus and the polarity of the classical receptive field. For example, a hypothetical, purely linear, on-center/off-surround neuron will display linear suppression when a white spot extends beyond the balance point of the classical center and the classical surround (Fig. 2, *B* and *D*, *point a*). By contrast, little or no linear suppression is evoked when the same linear neuron is stimulated with a sine-wave grating of the preferred spatial frequency (Fig. 2*E*). This is because the visual stimulus and the polarity of the classical receptive field closely match, regardless of the size of the visual stimulus (Fig. 2*F*). In the majority of neurons recorded in this study, the linear model predicts little or no surround suppression when using sine-wave stimuli with the preferred spatial frequency (Alitto and Usrey 2008), despite the finding that the same neurons show pronounced surround suppression when presented with sinusoidal stimulus at the preferred spatial frequency (Fig. 2*E*). It is this phenomenon—suppression exceeding the linear estimate—that is known as extraclassical, nonlinear surround suppression.

Although visual responses of an LGN neuron in the absence of nonlinear influences cannot be directly measured, they can be estimated from the linear DOG model obtained from the spatial frequency response function by convolving the linear estimate of the classical receptive field with the visual stimuli used to generate the area summation response function (Fig. 3). From this, the predicted influence of linear suppression on measured area summation response functions was quantified with the same suppression index shown above. For this analysis, only the spatial properties were considered; temporal properties were not included.

Modeling influence of nonlinear surround suppression on retinogeniculate and thalamocortical interactions. To estimate the influence of nonlinear surround suppression on retinogeniculate spike efficacy, we modeled LGN spike trains by weighting retinal spikes, recorded from the optic nerve during the presentation of stimuli that varied in size (details described above), according to their predicted efficacy

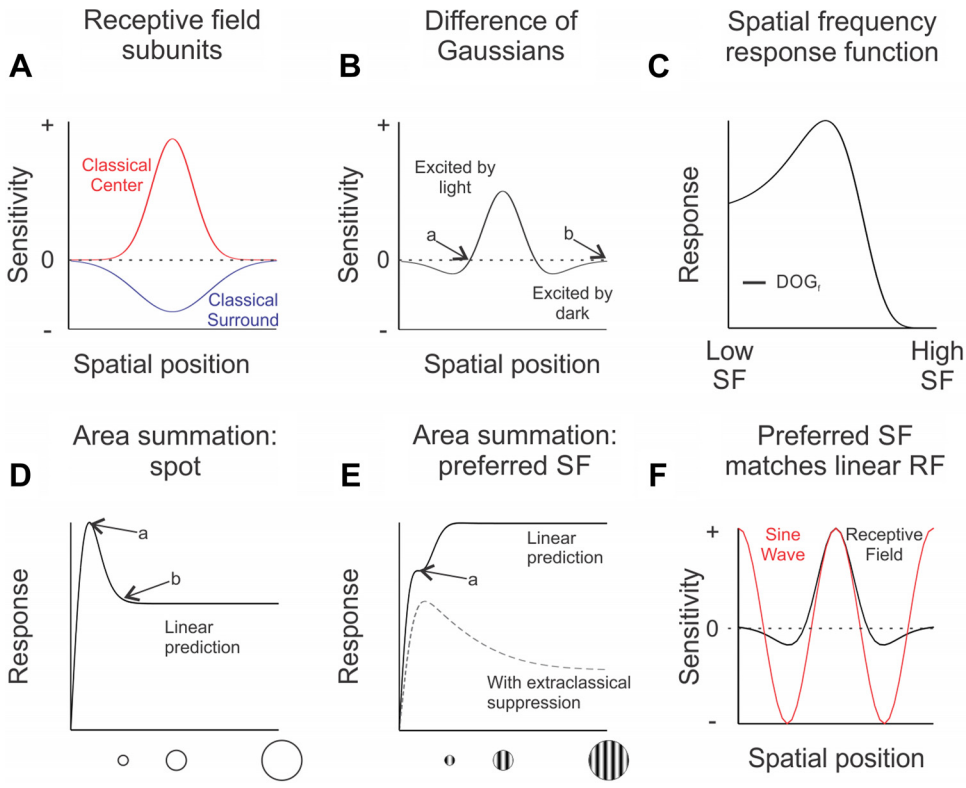

Fig. 2. Linear vs. nonlinear surround suppression. *A*: the classical center/surround receptive field has a circularly symmetrical, spatially antagonistic organization composed of 2 linear subunits: a classical center and a classical surround. *B*: the difference of Gaussians (DOG) model based on the linear combination of the classical center and surround subunits. *C*: when the DOG model is assumed, the spatial parameters can be estimated by fitting a spatial frequency (SF) response function to a frequency domain DOG equation (see MATERIALS AND METHODS). *D*: the response function of a hypothetical purely linear LGN neuron when presented with a spot of the preferred luminance polarity that varies in stimulus diameter. *E*: the response of the same hypothetical neuron to a sinusoidal grating of the preferred spatial frequency (solid black line; note that the decreased slope of the response at *point a* marks the transition point between the classical center and the classical surround: the point where the strength of the surround subunit equals the strength of the center subunit). In contrast to the hypothetical response, most LGN neurons display a substantial amount of nonlinear, extraclassical suppression that cannot be accounted for by the linear model (dashed gray line). *F*: the amount of predicted linear suppression to a sinusoidal stimulus depends on how well the spatial properties of the classical receptive field (RF) match the stimulus.

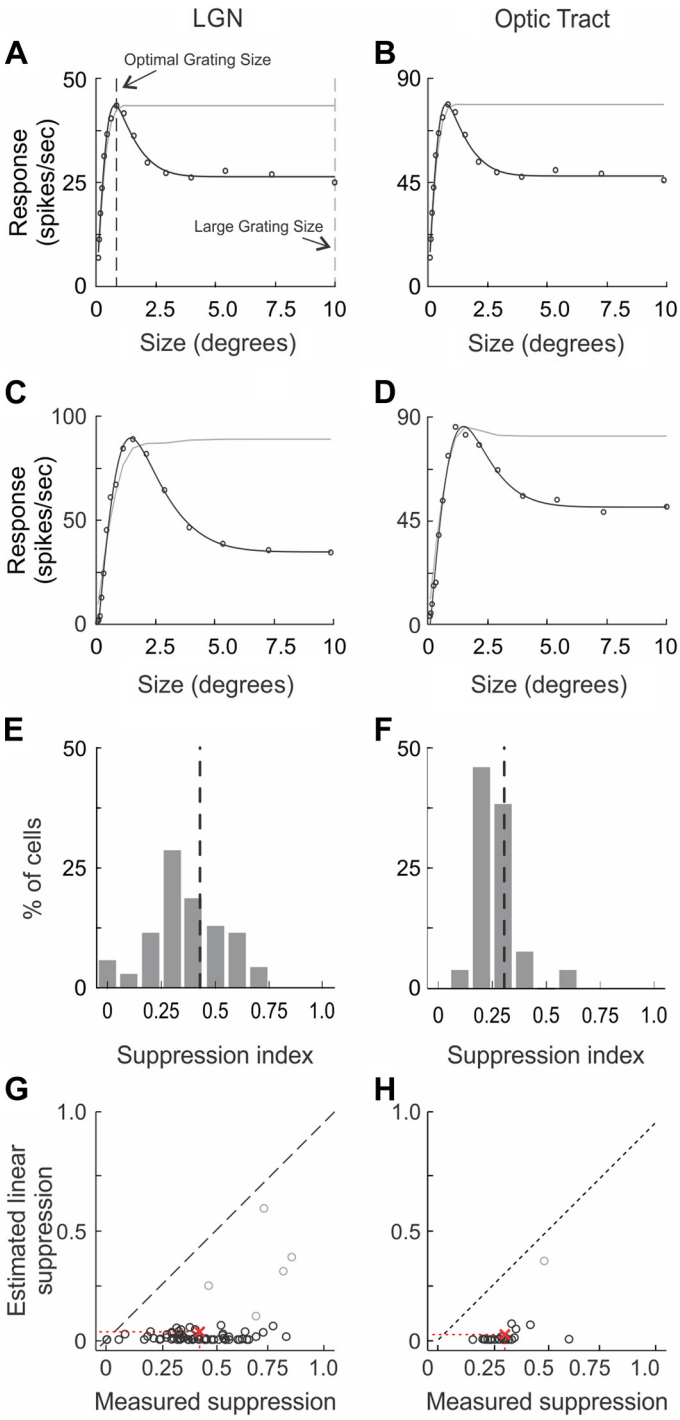

Fig. 3. Size tuning and extraclassical suppression in retinal ganglion cells and LGN neurons. Representative area summation response functions for 2 LGN neurons (*A* and *C*) and 2 retinal ganglion cells (*B* and *D*). Recordings of retinal ganglion cell activity made from the axons of retinal ganglion cells within the optic track. For each cell, the solid black line shows the DOG fit to measured values (black dots). *E* and *F*: histograms showing the distribution of suppression index values (see MATERIALS AND METHODS) for the sample of LGN neurons ($n = 81$) and retinal ganglion cells ($n = 28$). Dashed lines show the mean suppression index for the sample of LGN neurons and retinal ganglion cells (0.43 ± 0.02 and 0.30 ± 0.02, respectively; $P < 0.001$). *G* and *H*: scatterplots showing the relationship between measured suppression index values and suppression index values estimated for the linear contribution made by the classical surround of receptive fields (see MATERIALS AND METHODS). Red "X" indicates mean values.

based on previously published ISI-spike efficacy functions (Usrey et al. 1998), where efficacy equals the percentage of presynaptic spikes that evoke postsynaptic spikes. Because the efficacy of retinal spikes in evoking postsynaptic spikes is inversely related to the preceding ISI, retinal spikes following short ISIs were assigned higher weights than those following longer ISIs. For example, if 10% of retinal spikes with a preceding ISI of 20–22 ms and 20% of retinal spikes with a preceding ISI of 15–17 ms were reported to evoke LGN spikes, then these retinal spikes were assigned weights of 0.1 and 0.2, respectively. Firing rates for each stimulus diameter were then calculated by averaging across multiple repeats (3–5 repeats per stimulus diameter). Modeled LGN spike trains were transformed into area summation curves and analyzed in the same manner as the experimentally measured retinal and thalamic area summation curves. A similar model was created to estimate the influence of LGN surround suppression on the strength of geniculocortical communication using previously published ISI-spike efficacy functions for LGN neurons (Usrey et al. 2000).

Temporal frequency response functions. Temporal frequency response functions were calculated from neuronal responses to drifting sine-wave gratings (0.5–64 Hz, occasionally lower than 0.5 Hz, preferred spatial frequency, 100% contrast). Response curves were interpolated with a cubic spline to determine each neuron's preferred temporal frequency and the lowest and highest temporal frequencies to evoke a response 50% of maximum ($TF50_{low}$ and $TF50_{high}$, respectively). To determine the influence of surround suppression on the temporal frequency tuning properties of LGN neurons, temporal frequency response functions were generated with optimal-size drifting gratings (determined from area summation response functions, typically 1–2° diameter) and large gratings (~10° diameter) that extended into and beyond the extent of the suppressive surround. To examine the influence of surround suppression on the attenuation of responses to low temporal frequencies, we assessed low-frequency attenuation for both optimal-size and large stimuli, using the equation

$$\text{Low-frequency attenuation} = 1 - \frac{\text{Response}\left(\text{lowest temporal frequency examined}\right)}{\text{Response}\left(\text{preferred temporal frequency}\right)}$$

Time course and reliability of visual responses. To quantify the influence of surround suppression on the time course of visual responses, LGN neurons were excited with a nondrifting, sine-wave grating stimulus (100% contrast, optimal spatial frequency) that was modulated (180° phase shift) in time by an m-sequence of length $2^{15} - 1$. Specifically, the phase of the stationary grating changed by 180° each time the term of the m-sequence changed (from 1 to −1 or −1 to 1). The phases alternated between the cell's preferred phase and the null phase (180° shifted from preferred). The term of the m-sequence was updated every fourth refresh of the monitor (refresh rate = 140 Hz, 28.6 ms per term). This experiment was conducted twice, once with the optimal-size stimulus (typically 1–2° diameter) and once with a large stimulus (~10° diameter) that extended into and beyond the extent of the suppressive surround. Standard reverse-correlation analysis was performed on the spike trains evoked by both stimulus sets.

To quantify the influence of surround suppression on the reliability of LGN spikes, we presented many repeats (generally 50 or more) of a 3-s clip of the m-sequence-modulated, contrast-reversing stimulus (described above). Each presentation of the 3-s clip was followed by a 2-s interval of mean gray before the clip was repeated. Two sets of data were collected for each neuron, one using the optimal-size stimulus (typically 1–2 diameter) and one using a large stimulus that extended into and beyond the suppressive surround (~10° diameter). The Fano factor (spike count variance/mean spike count) was then calculated using the spike trains evoked by each stimulus set. The mean spike count and spike count variance were calculated with a sliding 30-ms window. The Fano factor was calculated for each time point, and the average value across the 3-s stimulus presentation was

used for further analysis. To determine whether or not a relationship between stimulus size and response reliability could be explained by changes in firing rate, we fit the spike count mean-to-variance relationship to a power function (variance = c*mean$\hat{n}$). This was done using the variance and mean values for each time bin (240, 30-ms bins for 3 s of stimulation). Fitting was done independently for each cell and both stimulus conditions (optimal-size stimulus and large stimulus).

Statistical analysis. When statistical analysis was performed to compare two distributions, we first used Lilliefors modification of the Kolmogorov-Smirnov test (Chakravarti et al. 1967) to determine whether the distributions in question were significantly different from normal distributions of unspecified mean and variance ($\alpha = 0.05$). If the distributions were not statistically different from normal, then a *t*-test was used to compare the means of the two samples; if the samples were statistically different from normal distributions, then a Wilcoxon rank sum test or a sign test was used. Although Y cells typically display greater nonlinear surround suppression than X cells (Shapley and Victor 1979b), classification of LGN neurons and retinal ganglion cells as X or Y type on the basis of response transience and latency (Usrey et al. 1999) did not influence the results (X cells = 61, Y cells = 15, unclassified = 5). Thus X and Y cells have been combined for all statistical analyses.

RESULTS

Strength of surround suppression in retina and LGN. To assess the strength of nonlinear surround suppression in the early visual system, we measured the spiking activity of 81 LGN neurons (layers A and A1) and 28 retinal ganglion cells (optic tract recordings) to drifting sinusoidal gratings as a function of stimulus size (4 Hz, 100% contrast, preferred spatial frequency). Because surround suppression increases with stimulus contrast (Bonin et al. 2005; Sceniak et al. 2006), all recordings were made while neurons were excited with high-contrast stimuli. Consistent with previous reports (Alitto and Usrey 2008; Murphy and Sillito 1987; Sceniak et al. 2006; Solomon et al. 2002; Webb et al. 2003), the firing rates of recorded neurons initially increased with stimulus size until a peak response was reached (Fig. 3, *A–D*). This increase in firing rate reflects a progressive increase in excitatory drive from the stimulus as the stimulus increased in size to fill both the classical center and the classical surround of the receptive field. Visual responses then decreased as the stimulus increased in size beyond the classical receptive field. This falling phase reflects the suppressive influence of the extraclassical or nonlinear surround—a region that extends beyond the cells' preferred size, where nonlinear suppressive mechanisms exceed linear excitatory mechanisms.

We quantified the strength of surround suppression using an index based on DOG fits to the area-summation response functions (see MATERIALS AND METHODS; DeAngelis et al. 1994; Jones et al. 2000; Sceniak et al. 1999). Across our sample of LGN neurons, there was a broad distribution of suppression index values, with nearly all neurons showing some degree of suppression (Fig. 3*E*). Suppression was also evident in our sample of retinal ganglion cells, albeit with a more restricted distribution of suppression index values (Fig. 3*F*). On average, the strength of surround suppression in the retina was ~70% of that in the LGN (mean suppression index: retina = 0.30 ± 0.02, LGN = 0.43 ± 0.02), a difference that was statistically significant ($P < 0.001$).

It is important to note that linear mechanisms from the classical surround can contribute to the falling phase of the area summation response function if there is poor spatial correspondence between the classical receptive field and the spatial frequency of the sine-wave grating used to measure neuronal responses (see MATERIALS AND METHODS for a detailed explanation). To determine the extent to which linear mechanisms influenced our measures of suppression, we first determined the spatial parameters of the classical receptive field (center and surround subunits) by fitting a DOG_f equation to each neuron's spatial frequency tuning curve. We then convolved the stimulus used for the area summation experiments with the estimated spatial profiles of the classical receptive field (see MATERIALS AND METHODS) to estimate the extent to which linear mechanisms contribute to surround suppression. The temporal kernel was not considered in this analysis. For the four neurons shown in Fig. 3, *A–D*, predicted area summation tuning curves based solely on spatial estimates of the classical receptive field displayed little or no suppression as stimulus size increased beyond the preferred. In contrast, the actual tuning curves (Fig. 3, *A–D*) for each neuron showed significant suppression as stimulus size increased beyond the preferred. With this method, linear suppression was found to make a minimal contribution to the total suppression observed experimentally in both the retina and LGN (Fig. 3, *G* and *H*; mean linear suppression index: retina = 0.02 ± 0.01, LGN = 0.03 ± 0.02). To minimize the contribution of linear suppression to our analyses, we excluded all neurons ($n = 6$) with linear suppression index values > 0.1 from further examination (Fig. 3, *G* and *H*, gray data points; likely the result of poor online estimation of preferred spatial frequency).

The finding that retinal surround suppression is ~70% of that measured in the LGN is consistent with the view that retinal mechanisms make a major contribution to LGN surround suppression (Alitto and Usrey 2008; Bonin et al. 2005; Solomon et al. 2006). With this in mind, we wished to know whether the feedforward influence from the retina may actually exceed 70% via synaptic and/or spike threshold mechanisms. We therefore performed an analysis to assess the strength of retinal suppression, taking into account the role of spike timing in retinogeniculate communication. Past work from several laboratories demonstrates that retinal spikes following short ISIs (<20 ms) are significantly more likely to evoke postsynaptic responses in the LGN compared with retinal spikes following longer ISIs (Levine and Cleland 2001; Mastronarde 1987; Rathbun et al. 2010; Sincich et al. 2007; Usrey et al. 1999; Weyand 2007). Because surround suppression lowers the average firing rate of retinal ganglion cells, it is reasonable to expect that it should shift their ISI distribution toward longer ISIs (i.e., less effective spikes). As a result, modeled area summation response functions that take into account retinal ISI should show a larger difference between responses to optimal-size stimuli and large stimuli.

To test the hypothesis that an ISI-based filter of retinogeniculate communication can increase the strength of surround suppression in the LGN, we passed each of the spike trains from our sample of ganglion cells through an ISI-based spike efficacy filter derived from physiological recordings previously published (Fig. 4*A*, *inset*; Usrey et al. 1998; see MATERIALS AND METHODS). As expected, lowering the firing rate of retinal ganglion cells through surround suppression shifted

the ISI distribution toward longer, less effective ISIs (Fig. 4, *A* and *B*). Importantly, the average spike evoked by an optimal-size stimulus had a greater likelihood of driving a postsynaptic spike (i.e., higher efficacy value; Cleland et al. 1971; Usrey et al. 1998, 1999) compared with the average spike triggered by a large stimulus (Fig. 4*C*; retinal spike efficacy: optimal-size stimulus = 14.6 ± 0.5%, large stimulus = 12.0 ± 0.6%, $P < 0.005$).

For each retinal ganglion cell in our sample, we next applied the efficacy filter to spikes comprising the full area summation response function and recalculated the suppression index (Fig. 4*D*). As predicted, the magnitude of surround suppression increased (Fig. 4*E*; mean suppression index: full spike train = 0.30 ± 0.02, ISI-filtered spike train = 0.36 ± 0.02; $P < 0.01$). Thus, when taking into account the influence of ISI on retinogeniculate interactions, feedforward mechanisms can account for an average of 84% of LGN extraclassical suppression.

These results indicate that one consequence of ISI on spike efficacy is to increase the contribution of feedforward mechanisms to LGN surround suppression. It is worth noting that this analysis was conducted on the spike trains of individual retinal ganglion cells, and LGN neurons in the cat are known to receive retinal input from one to four retinal ganglion cells (reviewed in Cleland 1986). Although all of the inputs to an LGN neuron have highly overlapping receptive fields and likely share similar size preferences (Usrey et al. 1999), a full account of the feedforward influence of ISI on surround suppression will require simultaneous recordings of all participating members of the circuit.

Given the significant influence that retinal ISI has on increasing the estimated strength of surround suppression in the LGN, we applied the same rationale to estimate the strength of surround suppression supplied from the LGN to V1 using an ISI-based spike efficacy filter previously reported for LGN cells with monosynaptic connections to simple cells in layer 4 of V1 (Fig. 4*F*, *inset*; Usrey et al. 2000). As with the retinal ganglion cells described above, surround suppression shifted the distribution of LGN spikes toward spikes with longer ISIs (Fig. 4, *F* and *G*). An analysis of the average efficacy of LGN spikes generated from optimal-size and large stimuli revealed that spikes occurring in response to a large stimulus were, on average, less effective than spikes occurring in response to an optimal-size stimulus (Fig. 4*H*; optimal-size stimulus = 3.8 ± 0.1; large stimulus = 2.9 ± 0.001; $P < 0.001$). Moreover, as with the retinogeniculate pathway, the influence of stimulus size on the distribution of LGN ISIs augmented the estimated magnitude of surround suppression propagated to V1 (Fig. 4, *I*

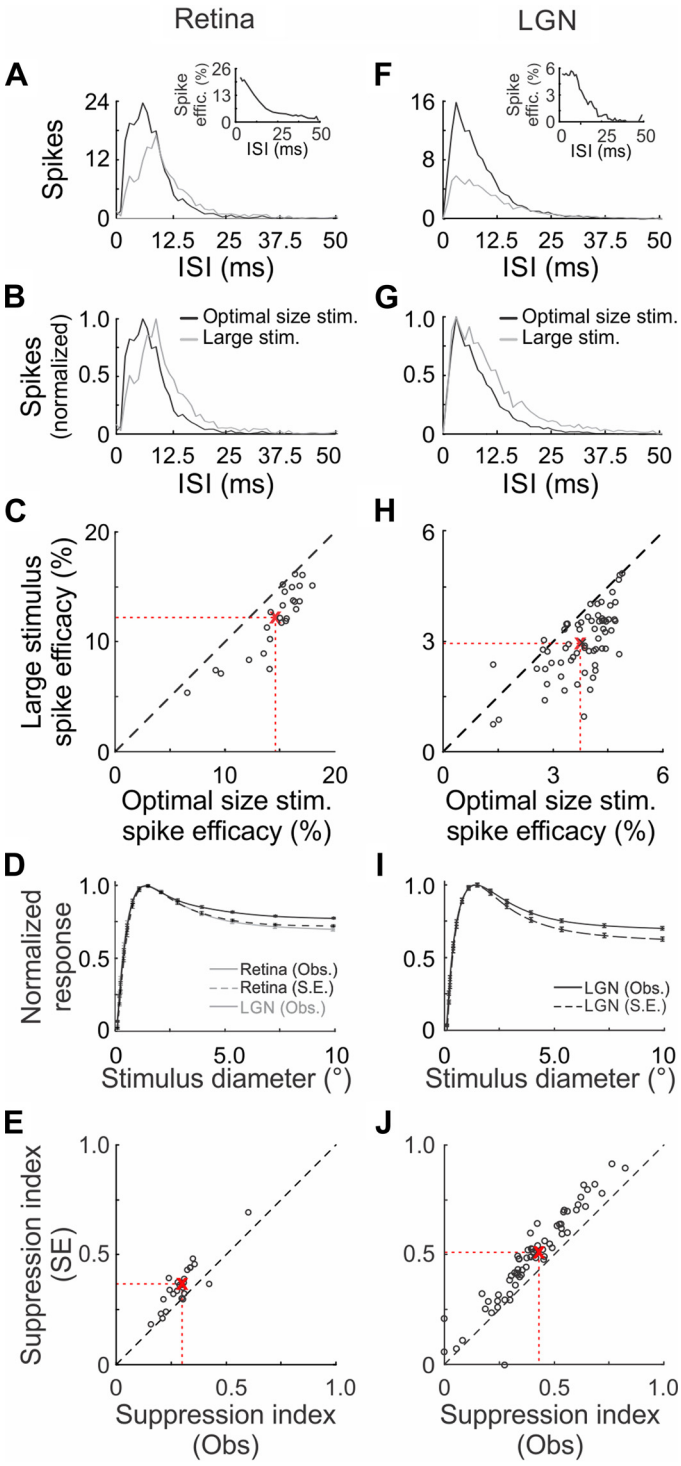

Fig. 4. Extraclassical suppression is amplified from presynaptic to postsynaptic neurons via stimulus size-dependent effects on the distribution of presynaptic interspike intervals (ISIs) and the relationship between ISI and synaptic efficacy. Compared with optimal-size stimuli, large stimuli shift the distribution of ISIs toward longer values. *A* and *B*: the distribution of ISIs for a representative retinal ganglion cell. *F* and *G*: the distribution of ISIs for a representative LGN neuron. Black lines show unnormalized (*A* and *F*) and normalized (*B* and *G*) responses to optimal-size stimuli; gray lines show responses to large stimuli. *A* and *F*, *insets*: the influence of ISI on the efficacy (% presynaptic spikes to evoke postsynaptic spikes) of retinogeniculate and geniculocortical communication (based on Usrey et al. 1998, 2000). At both locations in the visual pathway, efficacy is greatest for spikes following short ISIs. *C* and *H*: estimated average efficacy of retinal (*C*) and LGN (*H*) spikes evoked with large and optimal-size stimuli. Estimates based on the shift in ISIs with stimulus size and the relationship between ISI and efficacy (see MATERIALS AND METHODS). Red "X" indicates mean values. *D* and *I*: comparison of area summation response functions across cells calculated from experimentally observed values ("Obs," solid black lines) and values adjusted to take into account the influence of ISI and spike efficacy ("SE", dashed black lines) on synaptic communication. After accounting for suppression-dependent changes in spike efficacy, retinal area summation response functions are shifted toward the observed values for the LGN (*D*; gray line). *E* and *J*: using a suppression index to quantify the strength of surround suppression (see MATERIALS AND METHODS), the ISI-dependent enhancement of surround suppression from pre- to postsynaptic cells is significant ($P < 0.05$) for the pathway from retina to LGN (*E*) and from LGN to primary visual cortex (V1) (*J*). Red "X" indicates mean values.

and *J*; suppression index: full spike train = 0.41 ± 0.02, filtered spike train = 0.50 ± 0.03; $P < 0.01$).

Surround suppression and reliability of LGN responses. The ability of LGN neurons to transmit information from the retina to the cortex is also dependent on the variance of the responses to visual stimulation. Although visual neurons are often modeled as Poisson spike generators, response reliability, as measured by the Fano factor (variance/mean), is reported to increase as the mean firing rate increases (Kara et al. 2000). Consequently, the influence of surround suppression on firing rate could affect the reliability of LGN responses to visual stimulation. To test this prediction, we compared the Fano factor of LGN neurons ($n = 28$) excited with a repeating 3- to 5-s clip of an m-sequence-modulated, contrast-reversing, sine-wave grating stimulus presented at the optimal size and at a size that evoked maximal surround suppression (Fig. 5*A*).

Consistent with previous reports, the Fano factor of most cells was <1.0, indicating sub-Poisson statistics (optimal-size stimulus = 0.76, large stimulus = 0.82; Alitto et al. 2011; Kara et al. 2000). More importantly, there was a significant correlation between the change in Fano factor calculated from responses to optimal-size stimuli and large stimuli and the change in mean spike count (Fig. 5*B*; $r = -0.54$, $P < 0.005$). This correlation was significant regardless of the bin size of the window (5-1,000 ms) used to perform the analysis (Fig. 5*B* shows results with a 30-ms window). To quantify the relationship between surround suppression and response reliability further, we fit the spike count variance and spike count mean to a power function (Fig. 5, *C* and *D*). Results of this analysis show that the majority of LGN neurons have a power exponent < 1.0 (Fig. 5*D*). These findings indicate that as an LGN neuron is excited more robustly by the visual stimulus the Fano factor decreases, resulting in a statistically more reliable response. The change in Fano factor associated with the activation of surround suppression, however, can be accounted for by the corresponding change in firing rate. The best-fitting exponent of the power function was unchanged when the extraclassical surround was stimulated (Fig. 5*D*; optimal-size stimulus = 0.85 ± 0.01, large stimulus = 0.85 ± 0.02; $P = 0.56$). Thus, similar to other forms of response modulation, including contrast, orientation, and spatial attention (McAdams and Maunsell 1999; Tolhurst et al. 1981, 1983), surround suppression influences the reliability of visual responses without altering the fundamental relationship between spike count variance and mean.

Surround suppression, impulse response functions, and temporal frequency tuning. Mounting evidence, including the results described above, indicates that surround suppression in the LGN relies heavily on retinal mechanisms, including retinal contrast gain control (Bonin et al. 2005)—a phenomenon where neurons become less responsive to changes in stimulus intensity as stimulus contrast increases (Fig. 1; Shapley and Victor 1978). If so, then stimulation of the extraclassical receptive field should affect the temporal properties of neuronal responses in the LGN in a manner similar to increasing stimulus contrast. Specifically, visual responses in the LGN should become shorter in duration with surround suppression, and temporal frequency response functions should shift toward higher frequencies (as in Fig. 1). To test these predictions, we generated impulse response functions using noise-modulated, contrast-reversing, sine-wave grating stimuli of optimal and large size (see MATERIALS AND METHODS), and we calculated

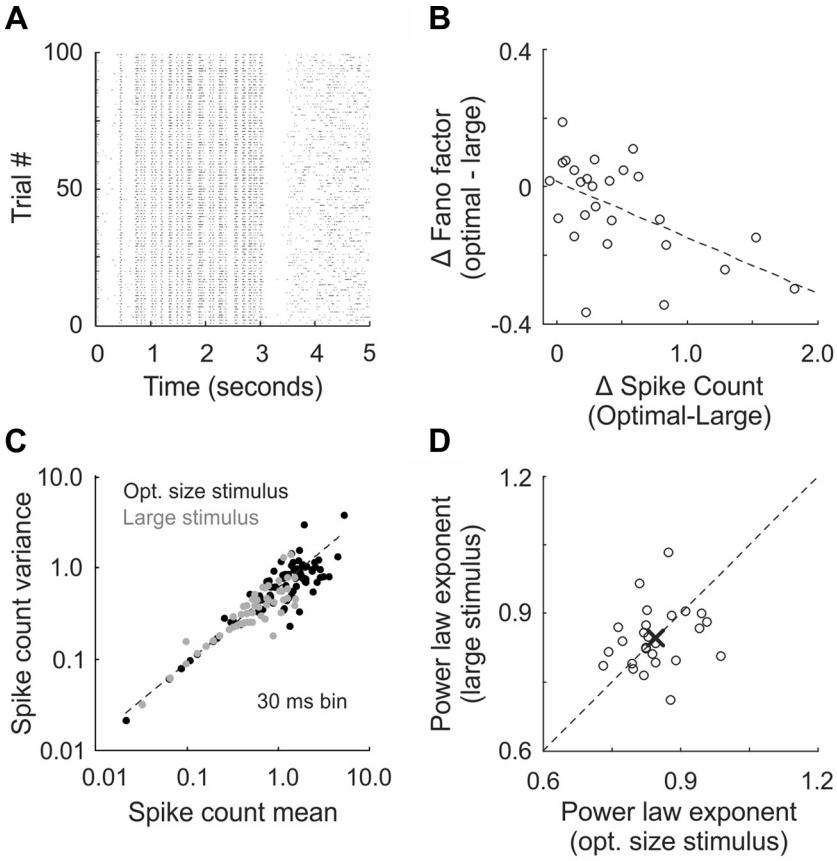

Fig. 5. Extraclassical suppression modulates LGN response reliability via changes in firing rate. *A*: raster plot showing the responses of a representative LGN neuron to repeated presentations of an optimal-size, 5-s clip of an m-sequence-modulated, contrast-reversing grating. The same sequence was also used for a large-size stimulus (data not shown). *B*: scatterplot showing the relationship between change in Fano factor (variance/mean) as a function of stimulus size and change in spike count. Across the sample of LGN neurons, there was a significant negative correlation (dashed line = linear regression). *C*: scatterplot showing the relationship between spike count variance and spike count mean for a representative cell stimulated with an optimal-size stimulus (black dots) and a large stimulus (gray dots). Each dot represents the mean and variance for a specific time bin of the 5-s stimulus using 30-ms bins. The values for the 2 stimulus conditions (large stimuli, optimal-size stimuli) were independently fit to power functions (dashed lines). *D*: across the sample of LGN neurons, surround suppression did not significantly influence the best-fitting power equation (X = mean value).

temporal frequency response functions using drifting gratings of optimal and large size.

We first examined the hypothesis that surround suppression modulates the temporal properties of LGN impulse responses. Consistent with the general view that the extraclassical surround serves to suppress visual responses, the magnitudes of the peak and rebound phases of impulse responses were significantly reduced when LGN neurons were stimulated with large stimuli compared with optimal-size stimuli (Fig. 6 and Fig. 7*A*; mean peak magnitude: large stimulus = 0.52 ± 0.06 spikes, optimal-size stimulus = 0.83 ± 0.08 spikes, $P < 0.001$; mean rebound magnitude: large stimulus = 0.52 ± 0.06 spikes, optimal-size stimulus = 0.82 ± 0.09 spikes, $P < 0.001$). More interestingly, there was a significant influence of surround suppression on the temporal properties of LGN impulse responses in a manner consistent with retinal contrast gain control. Namely, the duration of both the peak and rebound phases was significantly shorter when neurons were excited with the large stimulus compared with the optimal-size stimulus (Fig. 7*B*; peak phase duration: large stimulus = 46.9 ± 3.1 ms, optimal-size stimulus = 51.7 ± 3.2 ms, $P < 0.05$; rebound phase duration: large stimulus = 229.3 ± 30.8 ms, optimal-size stimulus = 355.5 ± 47.0 ms, $P < 0.05$).

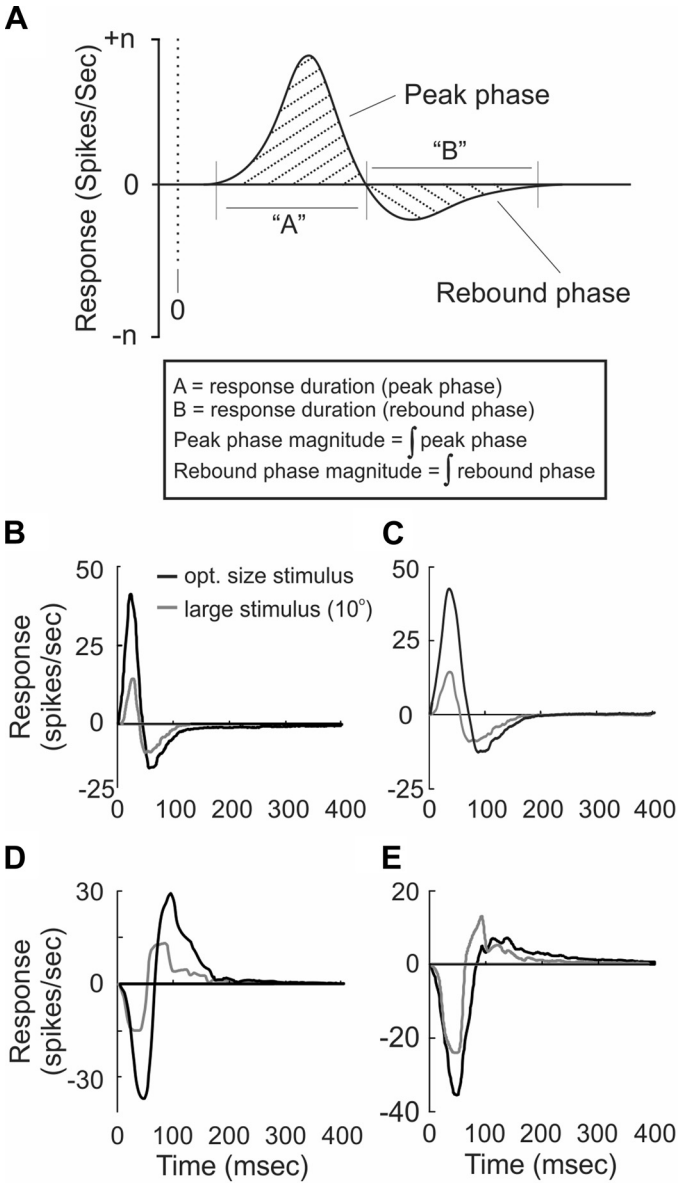

Fig. 6. Extraclassical suppression modulates the impulse response of LGN neurons. Impulse responses were calculated from neuronal responses to an m-sequence-modulated, contrast-reversing, sine-wave grating (see MATERIALS AND METHODS). *A*: schematic illustration of a typical impulse response. The biphasic response consists of an initial peak phase followed by a rebound phase. *B–E*: impulse responses from 4 representative LGN neurons: 2 on-center cells (*B* and *C*) and 2 off-center cells (*D* and *E*). For each cell, 2 impulse responses are shown, 1 with an optimal-size stimulus (black line) and 1 with a large stimulus that evoked extraclassical suppression (gray line).

Given that the impulse response is the inverse Fourier transformation of the response power spectrum, a decrease in the duration of the impulse response predicts a shift in the temporal frequency response function toward higher frequencies, a phenomenon also observed as a consequence of contrast gain control. To test this prediction, we used Fourier analysis to convert the impulse responses in our data set into temporal frequency response functions (Fig. 8, *A–C*). We also performed experiments to compare temporal frequency response functions generated from responses to large and optimal-size drifting gratings (Fig. 8, *D–F*). Both methods revealed a significant influence of surround suppression on the temporal frequency tuning properties of LGN neurons.

Extraclassical suppression modulated the temporal frequency tuning of LGN neurons in a manner similar to contrast gain control. Specifically, there was an increased attenuation of responses to low-frequency stimuli relative to high-frequency stimuli (Fig. 9*A*). Likewise, there was an inverse relationship between stimulus temporal frequency and the strength of extraclassical suppression (Fig. 9*B*). Extraclassical suppression also induced a significant rightward shift in the temporal frequency response functions of LGN neurons toward higher frequencies. This shift was evident in the lowest temporal frequency to evoke a half-maximum response ($TF50_{low}$; Fig. 9*C*; for contrast-reversing gratings: optimal size = 1.1 ± 0.1 Hz, large size = 1.7 ± 0.2 Hz, $P < 0.001$; for drifting gratings: optimal size = 0.7 ± 0.1 Hz, large size = 1.8 ± 0.3 Hz, $P < 0.001$) and the highest temporal frequency to evoke a half-maximum response ($TF50_{high}$; Fig. 9*D*; for contrast-reversing gratings: optimal size = 19.4 ± 2.0 Hz, large size = 19.9 ± 1.8 Hz, $P > 0.01$; for drifting gratings: optimal size = 20.1 ± 2.8 Hz, large size = 24.3 ± 2.9 Hz, $P < 0.01$).

DISCUSSION

The goal of this study was to determine the influence of nonlinear extraclassical surround suppression on temporal features of visual responses in the early visual system. Our results demonstrate that surround suppression is first established in the retina and then undergoes amplification in the LGN and layer 4 of V1 by mechanisms that include changes in the distribution of presynaptic ISIs and temporal summation of feedforward signals. Extraclassical suppression also influences LGN temporal integration in a manner qualitatively similar to retinal contrast gain control, decreasing the duration of LGN visual responses and causing a subsequent rightward shift in the temporal frequency response function. Collectively, these results indicate that feedforward inputs from the retina make a major contribution to the nonlinear receptive field properties of neurons in the LGN.

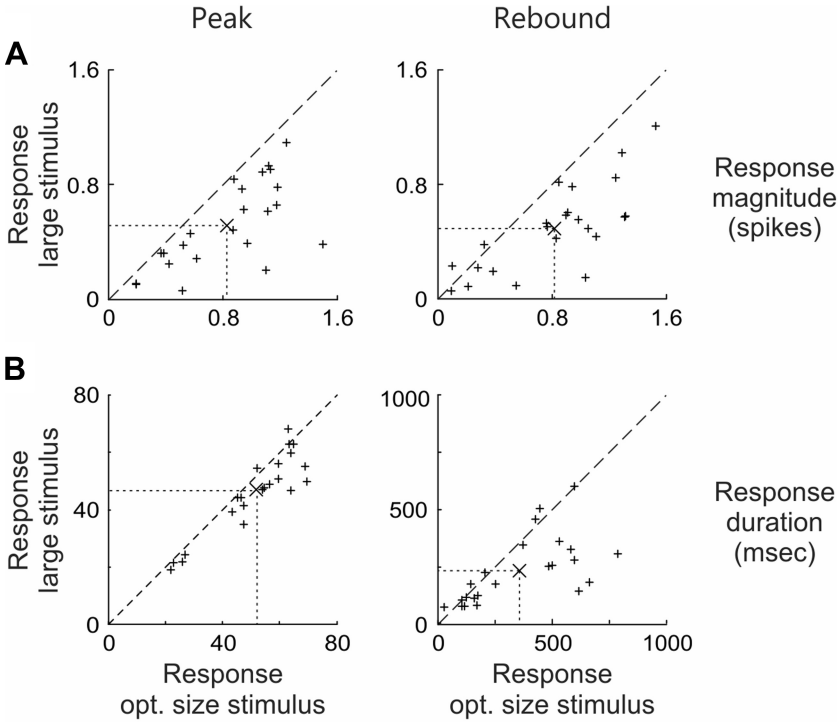

Fig. 7. Extraclassical surround suppression decreases the magnitude and duration of LGN impulse responses. Extraclassical surround suppression in the LGN decreases the magnitude (*A*) and the duration (*B*) of both the peak (*left*) and rebound (*right*) phases of LGN impulse responses. Cross hairs indicate mean values.

The neural origin of extraclassical suppression in the LGN has been a subject of considerable investigation, with studies providing evidence for involvement from corticogeniculate feedback (Andolina et al. 2013; Jones et al. 2012; Murphy and Sillito 1987; Nolt et al. 2007; Olsen et al. 2012) and recurrent thalamic inhibition (Cheng et al. 1995; Sclar 1987; Vaingankar et al. 2012; Webb et al. 2005). Here we show that retinal ganglion cells in the cat exhibit ~70% of the suppression measured in the LGN (Fig. 3). This agrees with previous reports demonstrating nonlinear surround suppression in retinal ganglion cells across a variety of species (Ahmed and Hammond 1984; Alitto and Usrey 2008; Caldwell and Daw 1978; Enroth-Cugell and Jakiela 1980; Nolt et al. 2007; Passaglia et al. 2001; Shapley and Victor 1979b; Solomon et al. 2006). Results from the present study also indicate that the contribution of feedforward mechanisms to nonlinear suppression in the LGN may be even greater than that described above, as the expression of retinal suppression is predicted to be amplified in the LGN via temporal summation and retinal spike efficacy mechanisms (Fig. 4). Feedforward contributions to extraclassical suppression are also indicated by previous results demonstrating that the onset of extraclassical suppression in the

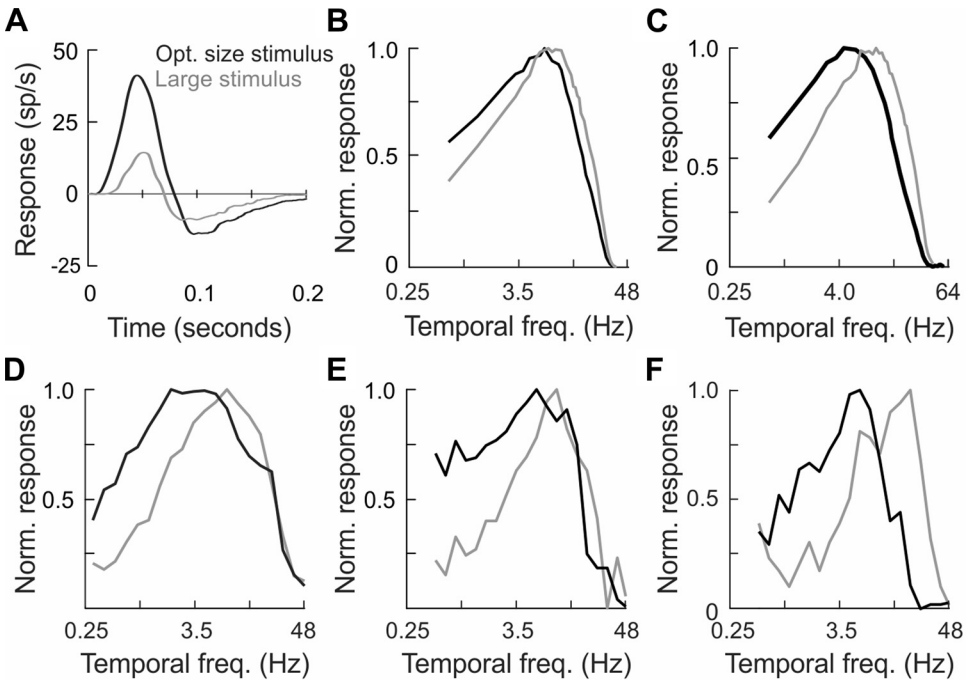

Fig. 8. Extraclassical surround suppression modulates temporal frequency tuning in the LGN. The influence of stimulus size on temporal frequency tuning is evident from measurements using contrast-reversing grating stimuli (*A–C*) and drifting grating stimuli (*D–F*). *A*: impulse response functions of a representative LGN neuron excited with an optimal-size stimulus (black line) and a large stimulus (gray line). *B* and *C*: temporal frequency response functions derived from the impulse responses of 2 representative LGN neurons (black lines, optimal-size stimuli; gray lines, large stimuli). Temporal frequency response functions were calculated by performing an inverse Fourier transformation on the impulse responses. *D–F*: temporal frequency response functions of 3 representative LGN neurons calculated directly from their responses to drifting sine-wave grating stimuli (black lines, optimal-size stimuli; gray lines, large stimuli) that varied in temporal frequency.

LGN is substantially faster than the response latency of corticothalamic feedback neurons in layer 6 of V1 (Alitto and Usrey 2008; Briggs and Usrey 2007). In addition, the tuning properties of LGN surround suppression more closely resemble the response properties of retinal ganglion cells than the response properties of V1 neurons (Bonin et al. 2005; Camp et al. 2009; Durand et al. 2007; Solomon et al. 2002). On the basis of these results, it appears that multiple mechanisms contribute to LGN surround suppression. Importantly, it is worth emphasizing that evidence demonstrating a role for one pathway does not negate involvement from other pathways. Rather, the existence of multiple mechanisms only further supports the assertion that surround suppression is an important strategy used by the brain to process visual information.

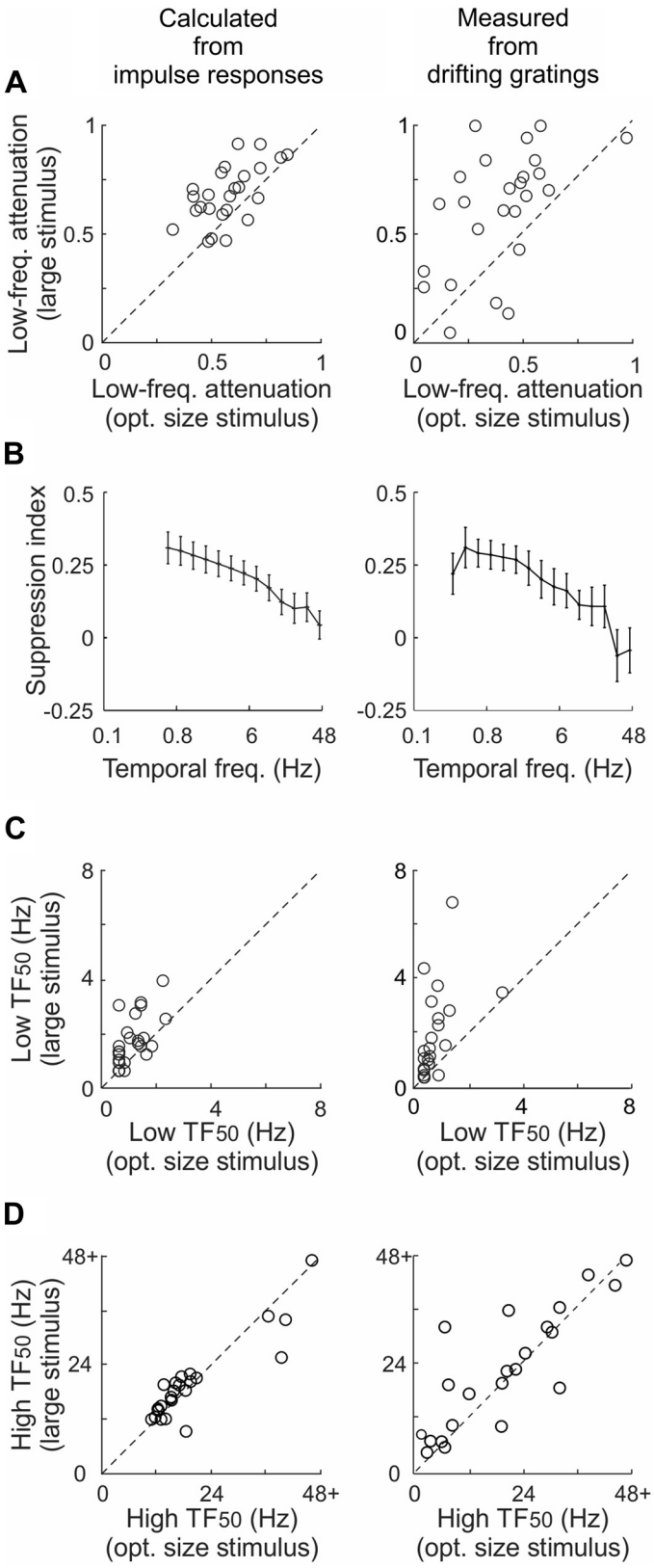

Fig. 9. Extraclassical surround suppression shifts LGN temporal frequency response functions toward higher frequencies. *A*: scatterplots showing the influence of stimulus size on low-frequency attenuation (see MATERIALS AND METHODS). Nonlinear suppression was greatest at low temporal frequencies, causing an increase in low-frequency attenuation in the LGN. *B*: line graphs showing the relationship between stimulus temporal frequency and the strength of suppression (quantified with a suppression index, larger values correspond to greater suppression; see MATERIALS AND METHODS) across the sample of LGN neurons. Suppression index values are inversely proportional to stimulus temporal frequency. Vertical lines indicate SE. *C* and *D*: the influence of extraclassical surround suppression on shifting temporal frequency response functions toward higher temporal frequencies is also evident in scatterplots showing a significant influence of stimulus size on the lowest (*C*) and highest (*D*) temporal frequencies to evoke half-maximum responses (Low TF50 and High TF50, respectively).

Previous work has suggested that extraclassical suppression in the retina and LGN can be explained as a manifestation of contrast gain control (Bonin et al. 2005; Mante et al. 2008; Shapley and Victor 1979b). One of the distinguishing features of contrast gain control is an inverse relationship between stimulus contrast and the gain of retinal ganglion cell and LGN cell responses, which leads to a saturating contrast response function (Alitto and Usrey 2004; Kaplan and Shapley 1986; Sclar 1987; Shapley and Victor 1978). In addition, contrast gain control decreases the gain at low temporal frequencies to a greater degree than the gain at high temporal frequencies and decreases the duration of impulse response functions (Benardete and Kaplan 1999; Lee et al. 1994; Shapley and Victor 1978, 1979a; Usrey and Reid 2000). With this is mind, it is noteworthy that results from the present study reveal that extraclassical suppression in the LGN decreases the duration of impulse response functions (Fig. 7) and has a greater suppressive influence with low-temporal frequency stimuli compared with high-temporal frequency stimuli (Fig. 9). These findings agree with previous work demonstrating that surround suppression decreases the duration of impulse response functions in the LGN (Benardete and Kaplan 1999; Mante et al. 2008; Solomon et al. 2010). Viewed from a broader perspective, the seemingly distinct phenomena of extraclassical suppression and contrast gain control can be unified by considering the balance of excitatory and inhibitory mechanisms involved in each. Typically, the organization of retinal and geniculate classical and extraclassical receptive fields is viewed as two overlapping fields, centered on the same spatial location. Whether the extraclassical receptive field is spatially more extensive than the classical receptive field is disputed (see Bonin et al. 2005), but this does not change the fundamental nature of the model. In the periphery of a receptive field an increase in stimulus size causes net suppression, while a more centrally located increase in contrast causes net excitation. As stimulus intensity increases, as a function of either contrast or diameter, the pool of recruited excitatory and inhibitory neu-

rons increases, decreasing the integration time of neurons in the early visual system, resulting in the observed changes in temporal response properties.

LGN surround suppression certainly influences cortical activity; however, it is unlikely to contribute directly to the full spatial extent of cortical extraclassical suppression (Angelucci and Bressloff 2006; Ozeki et al. 2009; Priebe and Ferster 2008). Although the magnitude of LGN suppression is comparable to values reported for V1 neurons (Cavanaugh et al. 2002; DeAngelis et al. 1994; Naito et al. 2007; Sceniak et al. 2001) and its influence is likely amplified via mechanisms that include the temporal filtering of feedforward signals (Fig. 4; see also Anderson et al. 2001), many features of extraclassical suppression in the LGN and V1 do not match (Ozeki et al. 2009). For instance, extraclassical suppressive fields are spatially much more expansive in V1 than in the LGN (Alitto and Usrey 2008; Bonin et al. 2005; Jones et al. 2000; Sceniak et al. 2001; Solomon et al. 2002; Webb et al. 2005). In particular, cortical extraclassical fields are two to five times the spatial extent of their corresponding classical receptive fields, whereas the same ratio in the LGN is between one and two times (Alitto and Usrey 2008; Bonin et al. 2005; Jones et al. 2000; Sceniak et al. 2001; Solomon et al. 2002; Webb et al. 2005). Moreover, results indicate that visual stimuli presented at the preferred size of a V1 neuron are sufficiently large to evoke maximal surround suppression from retinotopically aligned neurons in the LGN (Ozeki et al. 2004). In addition, unlike V1 extraclassical receptive fields, LGN extraclassical fields are not selective for stimulus orientation or direction, follow higher temporal frequencies, and display significantly less adaptation (Bonin et al. 2005; Durand et al. 2007; Girardin et al. 2002; Solomon et al. 2002; Webb et al. 2002; but see Naito et al. 2007). With these results in mind, there is evidence that LGN surround suppression may contribute to the near-surround (Ishikawa et al. 2010) and/or the high-contrast summation fields of V1 neurons (Angelucci and Sainsbury 2006; Ozeki et al. 2004). The more extensive surrounds of cortical neurons, however, likely rely on *1*) feedback from extrastriate areas, which can account for the correct spatial parameters and onset latencies of V1 suppression (Angelucci and Bressloff 2006; Bair et al. 2003; Nassi et al. 2013), and/or *2*) somatostatin-expressing local inhibitory neurons, the optogenetic inactivation of which blocks extraclassical suppression in mouse V1 (Adesnik et al. 2012; Nienborg et al. 2013).

Nonlinear suppression also modulates the response reliability of LGN neurons (Fig. 5), as measured by the Fano factor (variance/mean), causing a larger decrease in response mean than response variance. Importantly, though, the relationship between spike count variance and mean is not dependent on stimulus size; the best-fitting power equation was not influenced by the activation of surround suppression. Thus a neuron's response at a particular firing rate will have the same reliability regardless of whether it was generated by a suboptimal stimulus smaller than or larger than the preferred size. This general view agrees with past reports that the correlation between spike count mean and variance is unaltered by changes in stimulus parameters, such as contrast and orientation, or behavioral state, such as spatial attention (McAdams and Maunsell 1999; Tolhurst et al. 1981, 1983). The influence of surround suppression on response reliability can be explained by the relationship between mean spike count and response reliability. Traditionally, spiking activity has been modeled as a Poisson process (e.g., Shadlen and Newsome 1998); however, it has been established that a neuron's response reliability is directly related to the mean spike count (Churchland et al. 2010; Kara et al. 2000). As mean spike count increases, the variance tends to increase at an exponential rate <1.0, often resulting in responses at high firing rates that are more reliable than a Poisson process. Thus response reliability is fundamentally related to the amount of suprathreshold activity regardless of how that activity level was achieved.

Given the similarity between retinal and LGN receptive fields, it is interesting that the majority of synaptic input to LGN neurons comes from nonretinal sources (reviewed in Sherman and Koch 1986). In addition to corticogeniculate feedback and recurrent inhibition, surround suppression and retinal spike efficacy may also be modulated by cholinergic inputs, directly from the brain stem or indirectly from the basal forebrain via the thalamic reticular nucleus (De Lima and Singer 1987), which are reported to regulate LGN activity as a function of arousal (Steriade 2004) and spatial attention (McAlonan et al. 2008). With future experiments conducted in animals engaged in controlled behavioral tasks, it should be possible to determine the contribution of these modulatory inputs to the dynamic interactions between extraclassical surround suppression and visual processing in the temporal domain.

In summary, results from this study reveal a dynamic relationship between extraclassical surround suppression and temporal processing of visual signals. In particular, extraclassical suppression interacts with ISI-based mechanisms to adjust the strength of neuronal communication, an effect that serves to progressively amplify the magnitude of suppression in the retinogeniculocortical pathway. Extraclassical suppression also influences response reliability, the time course of impulse response functions, and the temporal frequency tuning of LGN neurons. Taken together, these results demonstrate that the extraclassical surround plays a major role in transforming temporal features of visual signals delivered to cortex.

ACKNOWLEDGMENTS

We thank Kelly Henning and Daniel Sperka for technical support.

GRANTS

This work was supported by National Eye Institute Grant EY-013588.

DISCLOSURES

No conflicts of interest, financial or otherwise, are declared by the authors.

AUTHOR CONTRIBUTIONS

Author contributions: H.J.A. and W.M.U. conception and design of research; H.J.A. and W.M.U. performed experiments; H.J.A. analyzed data; H.J.A. and W.M.U. interpreted results of experiments; H.J.A. and W.M.U. prepared figures; H.J.A. and W.M.U. drafted manuscript; H.J.A. and W.M.U. edited and revised manuscript; H.J.A. and W.M.U. approved final version of manuscript.

REFERENCES

Adesnik H, Bruns W, Taniguchi H, Huang ZJ, Scanziani M. A neural circuit for spatial summation in visual cortex. *Nature* 490: 226–231, 2012.

Ahmed B, Hammond P. Response of cat retinal ganglion cells to motion of visual texture. *Exp Brain Res* 53: 444–450, 1984.

Alitto HJ, Moore BD 4th, Rathbun DL, Usrey WM. A comparison of visual responses in the lateral geniculate nucleus of alert and anaesthetized macaque monkeys. *J Physiol* 589: 87–99, 2011.

Alitto HJ, Usrey WM. Influence of contrast on orientation and temporal frequency tuning in ferret primary visual cortex. *J Neurophysiol* 91: 2797–2808, 2004.

Alitto HJ, Usrey WM. Origin and dynamics of extraclassical suppression in the lateral geniculate nucleus of the macaque monkey. *Neuron* 57: 135–146, 2008.

Alitto HJ, Weyand TG, Usrey WM. Distinct properties of visually evoked bursts in the lateral geniculate nucleus. *J Neurosci* 25: 514–523, 2005.

Anderson JS, Lampl I, Gillespie DC, Ferster D. Membrane potential and conductance changes underlying length tuning of cells in cat primary visual cortex. *J Neurosci* 21: 2104–2112, 2001.

Andolina IM, Jones HE, Sillito AM. Effects of cortical feedback on the spatial properties of relay cells in the lateral geniculate nucleus. *J Neurophysiol* 109: 889–899, 2013.

Angelucci A, Bressloff PC. Contribution of feedforward, lateral and feedback connections to the classical receptive field center and extra-classical receptive field surround of primate V1 neurons. *Prog Brain Res* 154: 93–120, 2006.

Angelucci A, Sainsbury K. Contribution of feedforward thalamic afferents and corticogeniculate feedback to the spatial summation area of macaque V1 and LGN. *J Comp Neurol* 498: 330–351, 2006.

Ayaz A, Chance FS. Gain modulation of neuronal responses by subtractive and divsive mechanisms of inhibition. *J Neurophysiol* 101: 958–968, 2009.

Baccus SA, Meister M. Fast and slow contrast adaptation in retinal circuitry. *Neuron* 36: 909–919, 2002.

Bair W, Cavanaugh JR, Movshon JA. Time course and time-distance relationships for surround suppression in macaque V1 neurons. *J Neurosci* 23: 7690–7701, 2003.

Benardete EA, Kaplan E. The dynamics of primate M retinal ganglion cells. *Vis Neurosci* 16: 355–368, 1999.

Bonin V, Mante V, Carandini M. The suppressive field of neurons in lateral geniculate nucleus. *J Neurosci* 25: 10844–10856, 2005.

Briggs F, Usrey WM. A fast, reciprocal pathway between the lateral geniculate nucleus and visual cortex in the macaque monkey. *J Neurosci* 27: 5431–5436, 2007.

Caldwell JH, Daw NW. Effects of picrotoxin and strychnine on rabbit retinal ganglion cells: changes in centre surround receptive fields. *J Physiol* 276: 299–310, 1978.

Camp AJ, Tailby C, Solomon SG. Adaptable mechanisms that regulate the contrast response of neurons in the primate lateral geniculate nucleus. *J Neurosci* 29: 5009–5021, 2009.

Carandini M, Heeger DJ. Normalization as a canonical neural computation. *Nat Rev Neurosci* 13: 51–62, 2011.

Cavanaugh JR, Bair W, Movshon JA. Nature and interaction of signals from the receptive field center and surround in macaque V1 neurons. *J Neurophysiol* 88: 2530–2546, 2002.

Chakravarti HM, Laha RG, Roy J. *Handbook of Methods of Applied Statistics*. New York: Wiley, 1967, vol. I, p. 392–394.

Cheng H, Chino YM, Smith EL 3rd, Hamamoto J, Yoshida K. Transfer characteristics of lateral geniculate nucleus X neurons in the cat: effects of spatial frequency and contrast. *J Neurophysiol* 74: 2548–2557, 1995.

Churchland MM, Yu BM, Cunningham JP, Sugrue LP, Cohen MR, Corrado GS, Newsome WT, Clark AM, Hosseini P, Scott BB, Bradley DC, Smith MA, Kohn A, Movshon JA, Armstrong KM, Moore T, Chang SW, Snyder LH, Lisberger SG, Priebe NJ, Finn IM, Ferster D, Ryu SI, Santhanam G, Sahani M, Shenoy KV. Stimulus onset quenches neural variability: a widespread cortical phenomenon. *Nat Neurosci* 13: 369–378, 2010.

Cleland BG. The dorsal lateral geniculate nucleus of the cat. In: *Visual Neuroscience*, edited by Pettigrew JD, Sanderson KS, Levick WR. Cambridge: Cambridge Univ. Press, 1986, p. 111–120.

Cleland BG, Dubin MW, Levick WR. Simultaneous recording of input and output of lateral geniculate neurones. *Nat New Biol* 231: 191–192, 1971.

De Lima AD, Singer W. The brainstem projection to the lateral geniculate nucleus in the cat: identification of cholinergic and monoaminergic elements. *J Comp Neurol* 259: 92–121, 1987.

DeAngelis GC, Freeman RD, Ohzawa I. Length and width tuning of neurons in the cat's primary visual cortex. *J Neurophysiol* 71: 347–374, 1994.

Durand S, Freeman TC, Carandini M. Temporal properties of surround suppression in cat primary visual cortex. *Vis Neurosci* 24: 679–690, 2007.

Enroth-Cugell C, Jakiela HG. Suppression of cat retinal ganglion cell responses by moving patterns. *J Physiol* 302: 49–72, 1980.

Enroth-Cugell C, Robson JG. The contrast sensitivity of retinal ganglion cells of the cat. *J Physiol* 187: 517–552, 1966.

Felisberti F, Derrington AM. Long-range interactions modulate the contrast gain in the lateral geniculate nucleus of cats. *Vis Neurosci* 16: 943–956, 1999.

Georgeson MA. Temporal properties of spatial contrast vision. *Vision Res* 27: 765–780, 1987.

Girardin CC, Kiper DC, Martin KA. The effect of moving textures on the responses of cells in the cat's dorsal lateral geniculate nucleus. *Eur J Neurosci* 16: 2149–2156, 2002.

Hubel DH, Wiesel TN. Integrative action in the cat's lateral geniculate body. *J Physiol* 155: 385–398, 1961.

Ishikawa A, Shimegi S, Kida H, Sato H. Temporal properties of spatial frequency tuning of surround suppression in the primary visual cortex and the lateral geniculate nucleus of the cat. *Eur J Neurosci* 31: 2086–2100, 2010.

Jones HE, Andolina IM, Ahmed B, Shipp SD, Clements JT, Grieve KL, Cudeiro J, Salt TE, Sillito AM. Differential feedback modulation of center and surround mechanisms in parvocellular cells in the visual thalamus. *J Neurosci* 32: 15946–15951, 2012.

Jones HE, Andolina IM, Oakely NM, Murphy PC, Sillito AM. Spatial summation in lateral geniculate nucleus and visual cortex. *Exp Brain Res* 135: 279–284, 2000.

Kaplan E, Shapley RM. The primate retina contains two types of ganglion cells, with high and low contrast sensitivity. *Proc Natl Acad Sci USA* 83: 2755–2757, 1986.

Kara P, Reinagel P, Reid RC. Low response variability in simultaneously recorded retinal, thalamic, and cortical neurons. *Neuron* 27: 635–646, 2000.

Lee BB, Pokorny J, Smith VC, Kremers J. Responses to pulses and sinusoids in macaque ganglion cells. *Vision Res* 34: 3081–3096, 1994.

Levine MW, Cleland BG. An analysis of the effect of retinal ganglion cell impulses upon the firing probability of neurons in the dorsal lateral geniculate nucleus of the cat. *Brain Res* 902: 244–254, 2001.

Mante V, Bonin V, Carandini M. Functional mechanisms shaping lateral geniculate responses to artificial and natural stimuli. *Neuron* 58: 625–638, 2008.

Mastronarde DN. Two classes of single-input X-cells in cat lateral geniculate nucleus. I. Receptive-field properties and classification of cells. *J Neurophysiol* 57: 357–380, 1987.

McAdams CJ, Maunsell JH. Effects of attention on the reliability of individual neurons in monkey visual cortex. *Neuron* 23: 765–773, 1999.

McAlonan K, Cavanaugh J, Wurtz RH. Guarding the gateway to cortex with attention in visual thalamus. *Nature* 456: 391–394, 2008.

Murphy BK, Miller KD. Multiplicative gain changes are induced by excitation or inhibition alone. *J Neurosci* 23: 10040–10051, 2003.

Murphy PC, Sillito AM. Corticofugal feedback influences the generation of length tuning in the visual pathway. *Nature* 329: 727–729, 1987.

Naito T, Sadakane O, Okamoto M, Sato H. Orientation tuning of surround suppression in lateral geniculate nucleus and primary visual cortex of cat. *Neuroscience* 149: 962–975, 2007.

Nassi JJ, Lomber SG, Born RT. Corticocortical feedback contributes to surround suppression in V1 of the alert primate. *J Neurosci* 33: 8504–8517, 2013.

Nienborg H, Hasenstaub A, Nauhaus I, Taniguchi H, Huang ZJ, Callaway EM. Contrast dependence and differential contributions from somatostatin- and parvalbumin-expressing neurons to spatial integration in mouse V1. *J Neurosci* 33: 11145–11154, 2013.

Nolt MJ, Kumbhani RD, Palmer LA. Suppression at high spatial frequencies in the lateral geniculate nucleus of the cat. *J Neurophysiol* 98: 1167–1180, 2007.

Olsen SR, Bortone DS, Adesnik H, Scanziani M. Gain control by layer six in cortical circuits of vision. *Nature* 483: 47–52, 2012.

Ozeki H, Finn IM, Schaffer ES, Miller KD, Ferster D. Inhibitory stabilization of the cortical network underlies visual surround suppression. *Neuron* 62: 578–592, 2009.

Ozeki H, Sadakane O, Akasaki T, Naito T, Shimegi S, Sato H. Relationship between excitation and inhibition underlying size tuning and contextual response modulation in the cat primary visual cortex. *J Neurosci* 24: 1428–1438, 2004.

Passaglia CL, Enroth-Cugell C, Troy JB. Effects of remote stimulation on the mean firing rate of cat retinal ganglion cells. *J Neurosci* 21: 5794–5803, 2001.

Priebe NJ, Ferster D. Inhibition, spike threshold, and stimulus selectivity in primary visual cortex. *Neuron* 57: 482–497, 2008.

Rathbun DL, Warland DK, Usrey WM. Spike timing and information transmission at retinogeniculate synapses. *J Neurosci* 30: 13558–13566, 2010.

Rodieck RW. Quantitative analysis of cat retinal ganglion cell response to visual stimuli. *Vision Res* 5: 583–601, 1965.

Sceniak MP, Chatterjee S, Callaway EM. Visual spatial summation in macaque geniculocortical afferents. *J Neurophysiol* 96: 3474–3484, 2006.

Sceniak MP, Hawken MJ, Shapley R. Visual spatial characterization of macaque V1 neurons. *J Neurophysiol* 85: 1873–1887, 2001.

Sceniak MP, Ringach DL, Hawken MJ, Shapley R. Contrast's effect on spatial summation by macaque V1 neurons. *Nat Neurosci* 2: 733–739, 1999.

Scholl B, Latimer KW, Priebe NJ. A retinal source of spatial contrast gain control. *J Neurosci* 32: 9824–9830, 2012.

Sclar G. Expression of "retinal" contrast gain control by neurons of the cat's lateral geniculate nucleus. *Exp Brain Res* 66: 589–596, 1987.

Shadlen MN, Newsome WT. The variable discharge of cortical neurons: implications for connectivity, computation, and information coding. *J Neurosci* 18: 3870–3896, 1998.

Shapley R, Victor JD. The contrast gain control of the cat retina. *Vision Res* 19: 431–434, 1979a.

Shapley RM, Victor JD. The effect of contrast on the transfer properties of cat retinal ganglion cells. *J Physiol* 285: 275–298, 1978.

Shapley RM, Victor JD. Nonlinear spatial summation and the contrast gain control of cat retinal ganglion cells. *J Physiol* 290: 141–161, 1979b.

Sherman SM, Koch C. The control of retinogeniculate transmission in the mammalian lateral geniculate nucleus. *Exp Brain Res* 63: 1–20, 1986.

Sincich LC, Adams DL, Economides JR, Horton JC. Transmission of spike trains at the retinogeniculate synapse. *J Neurosci* 27: 2683–2692, 2007.

So YT, Shapley R. Spatial tuning of cells in and around lateral geniculate nucleus of the cat: X and Y relay cells and the perigeniculate interneurons. *J Neurophysiol* 45: 107–120, 1981.

Solomon SG, Lee BB, Sun H. Suppressive surrounds and contrast gain in magnocellular-pathway retinal ganglion cells of macaque. *J Neurosci* 26: 8715–8726, 2006.

Solomon SG, Tailby C, Cheong SK, Camp AJ. Linear and nonlinear contributions to the visual sensitivity of neurons in primate lateral geniculate nucleus. *J Neurophysiol* 104: 1884–1898, 2010.

Solomon SG, White AJ, Martin PR. Extraclassical receptive field properties of parvocellular, magnocellular, and koniocellular cells in the primate lateral geniculate nucleus. *J Neurosci* 22: 338–349, 2002.

Steriade M. Acetylcholine systems and rhythmic activities during the waking-sleep cycle. *Prog Brain Res* 145: 179–196, 2004.

Stromeyer CF 3rd, Martini P. Human temporal impulse response speeds up with increased stimulus contrast. *Vision Res* 43: 285–298, 2003.

Tadin D, Lappin JS, Blake R. Fine temporal properties of center-surround interactions in motion revealed by reverse correlation. *J Neurosci* 26: 2614–2622, 2006.

Tadin D, Lappin JS, Gilroy LA, Blake R. Perceptual consequences of centre-surround antagonism in visual motion processing. *Nature* 424: 312–315, 2003.

Tolhurst DJ, Movshon JA, Dean AF. The statistical reliability of signals in single neurons in cat and monkey visual cortex. *Vision Res* 23: 775–785, 1983.

Tolhurst DJ, Movshon JA, Thompson ID. The dependence of response amplitude and variance of cat visual cortical neurones on stimulus contrast. *Exp Brain Res* 41: 414–419, 1981.

Usrey WM. Spike timing and visual processing in the retinogeniculocortical pathway. *Philos Trans R Soc Lond B Biol Sci* 357: 1729–1737, 2002.

Usrey WM, Alonso JM, Reid RC. Synaptic interactions between thalamic inputs to simple cells in cat visual cortex. *J Neurosci* 20: 5461–5467, 2000.

Usrey WM, Reid RC. Visual physiology of the lateral geniculate nucleus in two species of New World monkey: *Saimiri sciureus* and *Aotus trivirgatis*. *J Physiol* 523: 755–769, 2000.

Usrey WM, Reppas JB, Reid RC. Paired-spike interactions and synaptic efficacy of retinal inputs to the thalamus. *Nature* 395: 384–387, 1998.

Usrey WM, Reppas JB, Reid RC. Specificity and strength of retinogeniculate connections. *J Neurophysiol* 82: 3527–3540, 1999.

Vaingankar V, Soto-Sanchez C, Wang X, Sommer FT, Hirsch JA. Neurons in the thalamic reticular nucleus are selective for diverse and complex visual features. *Front Integ Neurosci* 6: 118, 2012.

Webb BS, Tinsley CJ, Barraclough NE, Easton A, Parker A, Derrington AM. Feedback from V1 and inhibition from beyond the classical receptive field modulates the responses of neurons in the primate lateral geniculate nucleus. *Vis Neurosci* 19: 583–592, 2002.

Webb BS, Tinsley CJ, Barraclough NE, Parker A, Derrington AM. Gain control from beyond the classical receptive field in primate primary visual cortex. *Vis Neurosci* 20: 221–230, 2003.

Webb BS, Tinsley CJ, Vincent CJ, Derrington AM. Spatial distribution of suppressive signals outside the classical receptive field in lateral geniculate nucleus. *J Neurophysiol* 94: 1789–1797, 2005.

Weyand TG. Retinogeniculate transmission in wakefulness. *J Neurophysiol* 98: 769–785, 2007.